

# Notes

## Morphological Changes during the Annealing of Polybutene-1 Fiber

Joshua M. Samon,<sup>†</sup> Jerold M. Schultz,<sup>\*,†</sup> and Benjamin S. Hsiao<sup>\*,‡</sup>

Department of Chemical Engineering, University of Delaware, Newark, Delaware 19716, and Department of Chemistry, State University of New York at Stony Brook, Stony Brook, New York 11794

Received June 27, 2000

Revised Manuscript Received January 21, 2001

### Introduction

Polybutene-1 exhibits transient polymorphic behavior upon cooling from the molten state at atmospheric pressure. The polymer first crystallizes into a metastable tetragonal 11<sub>3</sub> helical form known as phase II. This metastable phase can transform into the stable hexagonal 3<sub>1</sub> helical form known as phase I.<sup>1</sup> The kinetics of this transformation has been shown to be influenced by pressure,<sup>2</sup> temperature,<sup>3</sup> and mechanical deformation<sup>4,5</sup> and has been studied extensively in the past via differential scanning calorimetry (DSC),<sup>6,7</sup> wide-angle X-ray scattering (WAXS),<sup>7,8</sup> and small-angle X-ray scattering (SAXS).<sup>9</sup>

Recent WAXS work by the authors<sup>10</sup> shows that the transformation kinetics and various structural properties (crystalline orientation and crystallinity index) of the fibers during room temperature annealing depend on the take-up speed at which the fibers were initially formed, the distinction being made between fibers spun at low (17 mpm) and high take-up speeds (100 and 250 mpm). A morphological model to explain the results was constructed, and it was suggested that at low take-up speeds the amorphous and crystalline components are connected in series. This morphology was thought to consist of small, isolated crystallites or rods of alternating crystalline–noncrystalline regions in a noncrystalline matrix. At higher take-up speeds a parallel connectivity was envisioned, consisting of interleaving shish kebab type structures. This model was consistent with the experimental findings that the orientation of the crystalline component relaxed in the case of the low take-up speed and increased in the case of the high take-up speed during annealing. In the first case the axial stress would be borne by the noncrystalline phase, and upon the release of stress the crystalline rods would lose orientation as the noncrystalline material relaxes. In the second case the axial stress would be borne by the crystals, and the noncrystalline material would relax within the crystalline bars or scaffolding. The present work is an extension of this study to directly investigate

the morphological changes of polybutene-1 during annealing at room temperature via SAXS.

### Experimental Section

**Materials.** The Shell Chemical Company donated the polybutene-1 resin, known as “polybutylene 4137”, used in this study. The resin had a  $M_w$  of 700 000 g/mol, a polydispersity index ( $M_w/M_n$ ) of 7.8, and a  $M_z$  of 2 500 000 g/mol. Its melting point was determined by DSC to be approximately 122 °C, and its glass transition temperature was approximately –23 °C.

**Experimental Procedure.** Fibers were spun using a 3/4 in. screw extruder with a temperature profile from feed zone to spinneret block of 180, 190, 195, and 195 °C. A 1/32 in. single hole spinneret die was used. The fibers were wound upon a take-up device, and samples were collected at take-up speeds of 30, 80, and 310 mpm. The extruder throughput was 2.15 g/min, achieved with a screw speed of 3.5 rpm.

Immediately after spinning (1 min of elapsed time), a small amount of fiber and the take-up spool were removed from the take-up device and quenched in liquid nitrogen. The liquid nitrogen retarded the morphological changes in the fibers. The quenched fibers were then transported to beamline X3A2 in the National Synchrotron Light Source (NSLS), Brookhaven National Laboratory (BNL), in Upton, NY. They were then removed from the liquid nitrogen and mounted in the X-ray beam and simultaneous SAXS and WAXS patterns were collected on imaging plates until near complete transformation of the phase II crystals to phase I crystals occurred.

### Results and Discussion

**SAXS.** Figure 1 shows representative SAXS patterns during the annealing process for fibers spun at take-up speeds of 30 and 310 mpm. Fibers spun at 80 mpm follow similar trends as the fibers spun at 30 mpm and will not be discussed further. For both cases, initially there is no lamellar structure apparent (the absence of meridional scattering lobes), and the only scattering signal present is that of an equatorial streak. As annealing progresses, scattering lobes become apparent near the beamstop along the meridian, while the equatorial streak remains unchanged.

The equatorial streak could arise from either needle-shaped voids or from microfibrils whose density is different from that of the surroundings. However, several previous studies suggest that the equatorial streak relates to the formation of microfibrils. Previous TEM investigations on highly oriented PB-1 thin films formed by melt-drawing show microfibrillar crystals, but no voiding.<sup>11–13</sup> Further, TEM images of poly(ethylene terephthalate) fibers at early stages of annealing show fibrils, but no voids, while the corresponding SAXS patterns exhibit an equatorial streak.<sup>14</sup> Finally, it has been suggested that if needle-shaped voids are created, this occurs as a response to the creation of microfibrils which are denser than the surrounding matrix.<sup>15</sup> A Guinier analysis of the equatorial streak reveals that the Guinier diameter of the 30 mpm fibers is  $99 \pm 6$  Å, and that of the 310 mpm fibers is  $99 \pm 17$  Å. This value corresponds very closely with the average diameter of

<sup>†</sup> University of Delaware.

<sup>‡</sup> State University of New York at Stony Brook.

\* To whom all correspondence should be addressed.

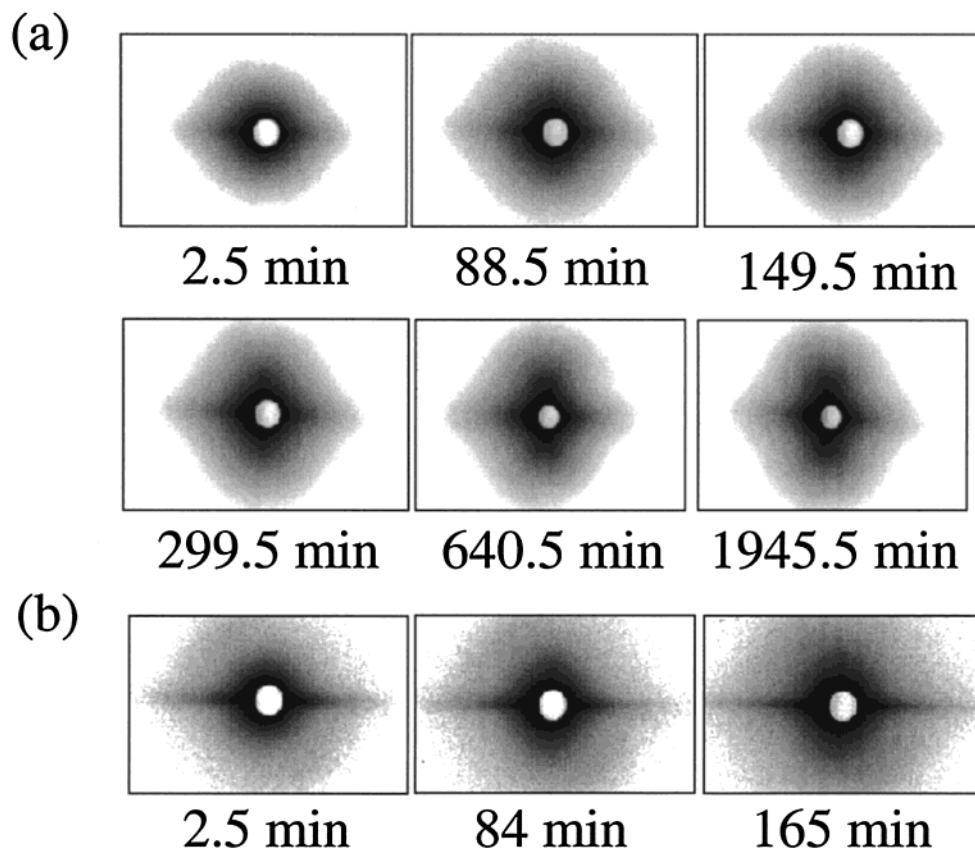


**Figure 1.** Two-dimensional SAXS patterns as a function of annealing time for fibers spun at a take-up speeds of (a) 30 mpm and (b) 310 mpm. The fiber axis is vertical.

100 Å found by Gohil et al.<sup>12</sup> in examining needlelike crystals in oriented thin films of polybutene-1 by transmission electron microscopy (TEM). This value was consistently found in examining films processed at different temperatures and with varying lengths of the needlelike crystals.

Figure 2 shows the Bragg spacing of these lamellar lobes as a function of annealing time. The Bragg spacing is initially at its maximum, and as annealing proceeds, it decreases asymptotically toward a constant value. The lamellar reflection appears soon after the start of annealing for the case of the fiber spun at 310 mpm, while it takes much longer for the 30 and 80 mpm fibers. Also, for the 310 mpm fiber the asymptotic value of the Bragg spacing is reached very quickly, whereas it takes many minutes for the case of the lower take-up speed.

The crystalline transformation kinetics was followed by analysis of the phase II (200) and the phase I (110) reflections in the WAXS patterns. Labeled patterns and the kinetic results are shown in Figure 3. There are large differences between the kinetics exhibited at 30 mpm as compared to those at 310 mpm, just as there were large differences between the 17 mpm fibers and the higher take-up speeds in the previous study.<sup>10</sup> These differences in the kinetics as a function of take-up speed arise from the increased effectiveness of the increased stress to aid in facilitating the axial motion of neighboring polymer chains in the crystallites. This motion would aid in the phase transition; the exact molecular process, however, is still unknown.

**Morphological Model.** For both high and low take-up speeds, immediately after spinning a fibrillar morphology is present, manifesting itself as an equatorial SAXS scattering streak. However, in the case of the 310

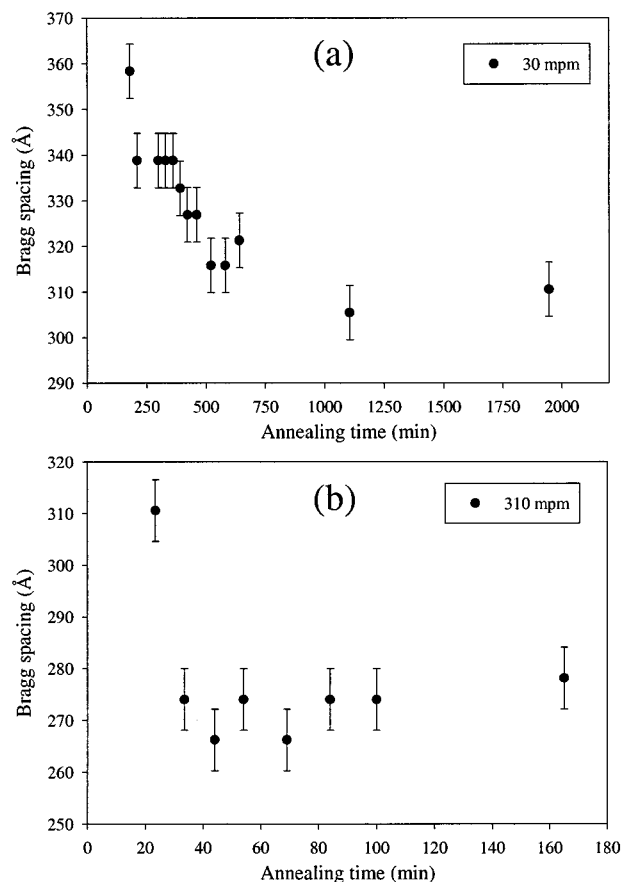


**Figure 2.** Bragg spacing of the lamellar peak as a function of annealing time for the (a) 30 and (b) 310 mpm fibers.

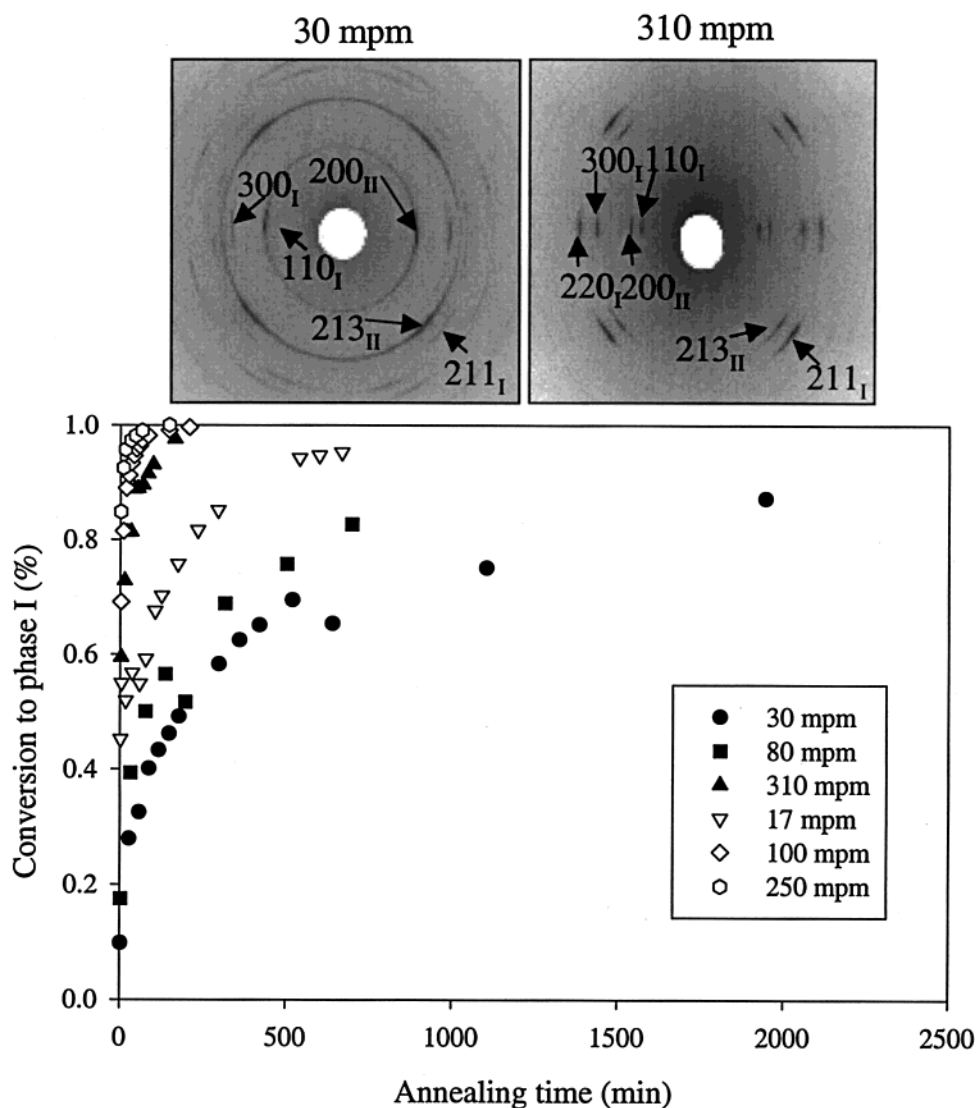


**Figure 3.** Percent conversion to phase I as a function of annealing time for both the present and past annealing study. Present results are shown in solid symbols, and the results of Samon et al.<sup>10</sup> are shown in open symbols. In addition, 2D WAXS patterns for take-up speeds of 30 and 310 mpm at the onset of annealing are shown, along with the corresponding indices of crystalline reflections.

mpm fibers, the SAXS equatorial streak is qualitatively much narrower in the direction parallel to the fiber axis, as compared to the 30 mpm fibers. The meridional breadth of the streak should increase with either decreasing length or increasing misorientation of the microfibrils. The two effects are not readily separated. Therefore, the microfibrils formed in the case of the high take-up speed must be significantly longer in the axial direction and/or possess better orientation as compared to the low take-up speed. This fact remains true throughout the annealing process. As the annealing progresses in both cases, lamellar lobes become evident, and by the end of the crystalline transformation the morphological transformation has also ended.

These results invalidate the previously proposed model because for all take-up speeds examined a rodlike morphology is present initially, which eventually transforms into a shish kebab morphology. The morphological distinction between low and high take-up speed therefore must not be the presence or absence of kebab growth but be the length and orientation of the rodlike crystals present. For low take-up speeds relatively short and/or low orientation microfibrils are present while for

the case of high take-up speeds longer and/or higher orientation microfibrils exist.

A parallel can be drawn between discontinuous fiber-reinforced composites and the present scenario. Composites made up of shorter or less oriented fibers have substantially different physical properties as compared to composites made up of longer or more oriented fibers. The properties of these long or more oriented fiber composites become similar to continuous fiber composites as the length of the fiber increases beyond the critical length for shear transfer from the matrix. In the present case, the low take-up speed fibers appear to behave like short fiber composites, and the high take-up speed fibers behave like continuous fiber composites. It is, however, not possible to make a quantitative test of this hypothesis at this time.

If this model is correct, then in the low take-up speed case little load would be transferred from the noncrystalline matrix to the crystals, and the noncrystalline material should dominate the mechanical behavior. The longer microfibrillar crystals in the high take-up speed case should bear most of the stress and should leave the noncrystalline material free to relax, while main-

taining the orientation of the microfibrils (the shish). This model is significantly different from our earlier suggestion that interleaving kebabs constitute a lattice-work which permits the crystal orientation to be maintained during annealing.

### Conclusions

The morphology exhibited by fibers spun at low and high take-up speeds shows both similarities and differences during annealing. In both cases a microfibrillar morphology gives rise to a shish kebab type morphology with similar fibrillar diameter. The length of the microfibrils or shish, however, increases with increased take-up speed. This result suggests a model in which fibers formed at low take-up speeds behave like short fiber composites, while fibers spun at high take-up speeds behave like continuous fiber composites. In this way, the mechanical behavior of fibers spun at low take-up speed is dominated by the matrix. Relaxation of the matrix would therefore disorient the crystals. Conversely, in fibers spun at higher speeds, the mechanical behavior is dominated by the shish moieties, and crystal disorientation is not possible.

**Acknowledgment.** The authors acknowledge the financial support of this work by NSF-GOALI Grant

DMR-9629825.

### References and Notes

- (1) Holland, V. F.; Miller, R. L. *J. Appl. Phys.* **1964**, *35*, 3241.
- (2) Nakafuku, C.; Miyaki, T. *Polymer* **1983**, *24*, 141.
- (3) Tanaka, A.; Sugimoto, N.; Asada, T.; Onogi, S. *Polym. J.* **1975**, *7*, 529.
- (4) Nakamura, K.; Aoike, T.; Usaka, K.; Janamoto, T. *Macromol.* **1999**, *32*, 4975.
- (5) Goldbach, G. *Makromol. Chem.* **1974**, *39*, 175.
- (6) Cortazar, M.; Sarasola, C.; Guzman, G. M. *Eur. Polym. J.* **1982**, *18*, 439.
- (7) Hsu, C. C.; Geil, P. H. *J. Macromol. Sci., Phys.* **1986**, *B25*, 433.
- (8) Nakafuku, C.; Miyaki, T. *Polymer* **1983**, *24*, 141.
- (9) Marigo, A.; Marega, C.; Cecchin, G.; Collina, G.; Ferrara, G. *Eur. Polym. J.* **2000**, *36*, 131.
- (10) Samon, J. M.; Schultz, J. M.; Hsiao, B. S.; Wu, J.; Khot, S. *J. Polym. Sci., Polym. Phys.* **2000**, *38*, 1872.
- (11) Gohil, R. M.; Miles, M. J.; Petermann, J. *J. Macromol. Sci., Phys.* **1982**, *B21*, 189.
- (12) Gohil, R. M.; Petermann, J. *J. Mater. Sci.* **1983**, *18*, 1719.
- (13) Petermann, J.; Schultz, J. M. *Colloid Polym. Sci.* **1984**, *262*, 217.
- (14) Chang, H.; Lee, K.-G.; Schultz, J. M. *J. Macromol. Sci.* **1994**, *B33*, 105.
- (15) Samon, J. M.; Schultz, J. M.; Hsiao, B. S.; Seifert, S.; Stribeck, N.; Gurke, I.; Collins, G.; Saw, C. *Macromolecules* **1999**, *32*, 8121.

MA001115Q